25th IMEKO TC4 International Symposium
23rd International Workshop on ADC and DAC Modelling and Testing
IMEKO TC-4 2022
Brescia, Italy / September 12-14, 2022

# Multiwavelet-based ECG compressed sensing with samples difference thresholding

Jozef Kromka, Ondrej Kovac, Jan Saliga, Linus Michaeli

*Technical University of Kosice, Letna 9, 04200 Kosice, Slovakia*
*e-mail addresses: {jozef.kromka, ondrej.kovac, jan.saliga, linus.michaeli}@tuke.sk*

***Abstract* – This paper introduces a novel Multiwavelet-based hybrid method of Compressed sensing (CS). A case study of CS and reconstruction of Electro Cardio Diagram (ECG) signals with the presented method was performed. For ECG signals the proposed method does not require a wave position detector and can reconstruct the signal with minimal DC offset error. The method is completely patient-agnostic and does not require prior patient-specific information as well. The proposed method was evaluated using the MIT-BIT database. The obtained results show a good reconstruction quality while keeping a high compression ratio.**

## I. INTRODUCTION

Remote health monitoring systems are becoming more important for doctors to perform long-term patient monitoring [1], [2]. They can help diagnose various health issues the patient may suffer with. One of the signals often measured by the remote health monitoring system is ECG. There are also others signals measured by the remote health monitoring systems [2], but the focus throughout this article will be on ECG signals.

Remote health monitoring systems are usually composed of nodes. Nowadays, the most significant specification which poses the challenge is power consumption. Since nodes often use wireless transmission to communicate and transmit data, this step is the most power-demanding [3]. By utilizing signal compression, the number of transmissions can be reduced, which would save energy. Used compression should not be computationally difficult because that would significantly increase power consumption [4]. Standard compressions are performed by sampling the signal according to Shannon's theory. This signal is often processed to remove redundancy by decorrelation. Then only a few coefficients from the transformed signal need to be transmitted. This approach showed a good compression efficiency with a low error after reconstruction. But the standard compressions also have several drawbacks. For example, matrix multiplication which is used to perform transformation is power-demanding [5]. The compression which utilizes transformation works by prioritizing low-frequency components of the signal over high-frequency components [6]. Compressed sensing [7] is a novel method of compression, which is not power-demanding as the standard compression methods [8]. It performs the compression directly while acquiring the signal. CS utilizes the signal sparsity to achieve sufficient compression and signal reconstruction at the sub-Shannon sampling rate. These properties of CS can be used to lower power consumption in remote health monitoring systems.

In recent years, various methods for the application of CS directly to ECG signals were proposed. A hybrid encoding algorithm for real-time CS acquisition of ECG signals was introduced in [9]. The algorithm can be used for efficient ECG acquisition with a reduced computational load on the compressor. Dictionary-based CS reconstruction method was introduced in [10]. A novel approach for the optimization of a dictionary, which is used in ECG signal reconstruction was proposed. The results showed this dictionary can increase performance, over the standard trained dictionaries, due to lower redundancy. But these methods use the R peak detector which requires additional logic and computational power. In [11] a new greedy algorithm was proposed. This algorithm requires the support information about the signal to improve reconstruction quality. ECG CS method with high compression ratio and dynamic model reconstruction was proposed in [12], [13]. This method uses a QRS detector to detect the exact R wave position for signal segmentation before compression. The drawback of this method is that it requires the R peak detector and that it introduces a DC offset error to the signal between the frames.

The proposed algorithm is based on Multiwavelets and a novel approach of CS sampling. The method was evaluated on ECG signals. For ECG signals this approach of CS does not require a wave position detector and can reconstruct the signal with minimal DC offset error. The method is completely patient-agnostic and does not require prior patient-specific information as well.

The article is organized as follows: The second section introduces the theoretical background of CS and Discrete Multiwavelet transform (DMWT). The third section describes proposed CS sampling, and signal reconstruction algorithms. In the fourth section, the performance of the new algorithm was assessed using the MIT-BIH arrhythmia database. Finally, the conclusion and direction of future works are presented in the last section.

## II. THEORETICAL BACKGROUND

In this section, the theoretical background of CS is explained. The basic theory of DMWT, used as the basis for sparse signal recovery, is presented in the latter part of this section.

### *A. Compressed sensing theory*

CS assumes that the signal can be represented by only K nonzero coefficients with a suitable basis, where K is much smaller than the signal length. This signal is called a sparse signal. Usually, the signals are sparse on some orthogonal basis [11]. Some signals do not show sparsity with an orthogonal basis. In that case, a dictionary basis [10] can be used to sparsify the signals. In both cases, the sparse representation of a signal can be obtained according to (1)

$$f = \psi x, \tag{1}$$

where $f$ is a signal with length N, $\psi$ is a N × N basis matrix, and $x$ is the sparse representation of the signal. The sparse representation of the signal has length N, but only K coefficients are nonzero values.

In CS, the signal is sampled not uniformly like in common signal acquisition methods. The signal is sampled according to the measurement matrix. The sampling can be defined by the following equation (2)

$$y = \phi f, \tag{2}$$

where $y$ is a compressed measurement with length M, $\phi$ is the M × N measurement matrix, and $f$ is the signal with length N.

If the signal $f$ is sparse on some basis, and K < M << N, then the compressed measurement $y$ contains enough information to reconstruct the signal $f$. The signal is reconstructed according to (1). The sparse representation of the signal can be obtained by substituting the signal $f$ in (2) by expression (1) forming the following equation (3)

$$y = \phi\psi x. \tag{3}$$

One of the requirements to be able to obtain the sparse solution to (3) is that the measurement matrix must be incoherent with the basis matrix. In other words, rows of measurement matrix can not sparsely represent the columns of the basis matrix [15]. Incoherency can be achieved by constructing the measurement matrix in a way that the signal is sampled at random places.

Usually, in (3) the measurement and the basis matrix are substituted with the reconstruction matrix $A$. The reconstruction matrix can be obtained according to (4)

$$A = \phi\psi. \tag{4}$$

The size of the reconstruction matrix is M × N. By substituting the basis and the measurement matrix by (4) in (3) following equation (5) is obtained

$$y = Ax. \tag{5}$$

The equation (5) is used to find the sparse representation of the signal for the compressed measurement. Since there are N unknowns and M equations, and N > M, this system of equations is an undetermined system of linear equations.

The solution to the undetermined system of linear equations is usually based on minimalization according to (6)

$$\min_{x\in\mathbb{R}^n} \|x\|_p, \qquad subject\ to\ y = Ax, \tag{6}$$

where $\|-\|_p$ indicates $l_p$ norm. Initially, an $l_0$ norm was proposed in [7]. But among all possible norms, the $l_0$ norm is polynomial-time hard, highly unstable and the solution can be found only by brute force methods [13]. Thus using the $l_1$ norm was proposed in [16]. The $l_1$ norm problems can be solved by convex optimization algorithms, or by greedy algorithms. One difference between the algorithms is that greedy algorithms are suboptimal. Another difference is that they can reach an almost optimal solution with a lower number of computations compared to convex optimization algorithms [17]. The greedy algorithms usually require prior knowledge of how much the signal is sparse. The convex optimization algorithms do not require this prior information. The most used convex optimization algorithm is the basis pursuit algorithm [15]. The most used greedy algorithms are Orthogonal Matching Pursuit (OMP), Compressive sampling matching pursuit (CoSaMP), and Iterative Hard Thresholding (IHT) [15].

### *B. Discrete Multiwavelet transform*

DMWT was developed as the result of the advancement in the development of Discrete Wavelet transform (DWT) and Wavelet theory. The main difference between DMWT and DWT is that DWT uses only one scaling and one wavelet function to approximate the signal, while DMWT can use up to $r$ scaling and $r$ wavelet functions. In the DMWT case, these functions are called multiscaling and multiwavelet functions. The advantage of DMWT over DWT is that the multiscaling and multiwavelet function has compact support, high smoothness, and high approximation order. Multiscaling and multiwavelet functions are symmetric as well as orthogonal [18]. They are represented as vectors according to (7)

$$\begin{aligned} \varphi &= (\varphi_1, \dots, \varphi_r)^T \\ \psi &= (\psi_1, \dots, \psi_r)^T, \end{aligned} \tag{7}$$

where $\varphi$ is the multiscaling function, $\psi$ is the multiwavelet function, $r$ is the multiplicity of multiscaling and multiwavelet function, and $T$ means transpose. As in the DWT case, these functions are not defined as shown in (7), but rather in the form of an impulse response. In the DMWT case, these impulse responses are defined as matrices with the size $r \times r$. In general $g_0(0) \dots g_0(n)$ are the matrix impulse responses of multiscaling functions and $g_1(0) \dots g_1(n)$ are the matrix impulse responses of wavelet functions.

Multiwavelets used in the presented method are Donovan-Geronimo-Hardin-Massopust (DGHM), BAT,

Chui – Lian (CL), Daubechies (DB), Symmetric Asymmetric of order 4 (SA4), and Haar Multiwavelet. These Multiwavelets were selected because they can be easily found in literature as well as they are implemented and ready to use in the following Multiwavelet toolbox [19]. The matrix impulse responses of these Multiwavelets with the corresponding literature can be found in [18].

To use DMWT as a basis for CS, the basis matrix needs to be constructed. The Multiwavelet basis matrix can be constructed similarly to the Wavelet basis matrix [20]. The Wavelet scalar impulse responses are replaced by the matrix impulse responses of Multiwavelets. The basis matrix then can be constructed according to (8). It is also important to keep in mind, that the constructed matrix will be $r$ times bigger after substituting the coefficients of matrix impulse responses, into the designed basis matrix

$$U=\begin{bmatrix} g_0(n) & g_0(n-1) & \dots & g_0(0) & \dots & 0 \\ g_1(n) & g_1(n-1) & \dots & g_1(0) & \dots & 0 \\ 0 & 0 & g_0(n) & g_0(n-1) & \dots & g_0(0) \\ 0 & 0 & g_1(n) & g_1(n-1) & \dots & g_1(0) \end{bmatrix}. \quad (8)$$

The basis matrix can be constructed in another way by using the DMWT on the columns of the identity matrix and rearranging the coefficients. With this approach, it is also possible to construct a multilevel Multiwavelet basis matrix. For the multilevel Multiwavelet basis matrix, multilevel DMWT should be applied to the columns of the identity matrix. The implementation of the DMWT and multilevel DMWT can be found in [19].

## III. THE PROPOSED CS ALGORITHM

This section presents a novel hybrid method of CS. The section is split into two parts. The proposed method of CS on the transmitter side is introduced, in the first part. Subsequently, the reconstruction algorithm is explained in the following subsection. To perform DMWT and to construct the basis, a Multiwavelet toolbox for MATLAB was used [19]. To find the sparse solution according to equation (5) in the proposed signal reconstruction method, the CVX package for specifying and solving convex programs was used [21].

### *A. CS performing*

The block diagram of the proposed ECG compression algorithm is outlined in Fig. 1. The ECG signal is acquired at the sampling frequency $f_S$ and split into frames with constant length $N$. From the frame, DC offset is removed and saved to the data block. The frame $f[n]$ is then filtered with the multiscaling impulse responses of chosen Multiwavelet. This filtration is performed $L$ times, achieving $L^{\text{th}}$ level of DMWT transform for only multiscaling coefficients. These multiscaling coefficients $c_{1,2}$ with respective length $N/2^L$ are stored for quantization and encoding as well as filtered with the inverse multiscaling impulse responses of chosen Multiwavelet. This filtration is also performed $L$ times, achieving $L^{\text{th}}$ level of inverse DMWT transform. The resulting signal will present the low-frequency component of the ECG signal. Low-frequency component ECG signal is then removed from the original ECG signal. After removal, a high-frequency component ECG signal is obtained.

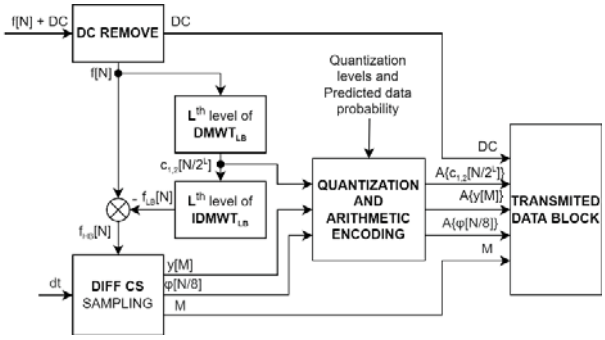


*Fig. 1. Block diagram of CS ECG signal acquisition*

The high-frequency component of ECG will be input to the block which performs the Samples Difference Thresholding. (SDT). SDT block performs the CS sampling and constructs the sensing matrix, used for the signal reconstruction. The SDT block computes the difference between the two samples, and if the difference is higher than the defined constant $dt$ then the latter sample is stored in a compressed measurement signal, and the position is stored in the sensing matrix. If the difference is less than $dt$ then only zero is stored in the sensing matrix. The SDT block also keeps track of the size of the compressed measurement signal. The SDT would never sample the first sample of the frame as well as it cannot evaluate the difference between the last sample and the first sample of the following frame. That is why the first and the last sample are stored automatically. The size of the compressed measurement signal is then directly stored in the data block. Compressed measurement signal $y$, together with the sensing matrix $\phi$ and the multiscaling coefficients $c_{1,2}$ are then quantized and encoded with the arithmetic encoding. A linear quantization with a defined number of quantization levels was used. While evaluating the method, it was found that the histogram of the Compressed measurement signal and multiscaling coefficients is resembling the Gauss function. This information is used while performing the arithmetic encoding. The sensing matrix is stored in a form of a binary number with N bits. The binary number is then divided into the binary array with a length of 8 forming 8-bit numbers. These 8-bit numbers are also encoded with the arithmetic encoder because they have big redundancy. DC offset, compressed measurement signal, length of the compressed measurement signal, multiscaling coefficients, and sensing matrix are then stored in the data block.

### *B. CS reconstruction*

The reconstruction method is outlined in Fig. 2. The

method is slightly different from the basic CS signal reconstruction. All data from the transmitted data block are decoded and then dequantized.

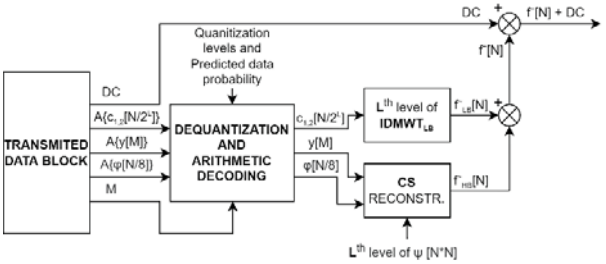


*Fig. 2. Block diagram of ECG signal reconstruction*

The compressed measurement signal, with the signal length and measurement matrix are used to reconstruct the high-frequency component of the ECG signal. The multiscaling coefficients are used to restore the low-frequency component of the ECG signal. The low-frequency and the reconstructed high-frequency component are then combined. In the end, the DC offset is restored and the final reconstructed ECG frame is obtained.

## IV. EXPERIMENTAL RESULTS

The proposed method was evaluated in the MATLAB environment using the MIT-BIH arrhythmia database [14] as a set of test ECG signals. The database contains 48 ECG records sampled at 360 Hz with 11-bit resolution. To evaluate the compression ratio (CR) of the proposed method following equation (9) was used

$$CR = \frac{N\mathrm{B}_0}{D}. \qquad (9)$$

In equation (9), $N$ is the frame length, $\mathrm{B}_0$ is the bit resolution of the original signal, which is 11 in the case of the MIT-BIH database. The $\mathrm{D}$ represents the number of bits in the transmitted data block. The number of transmitted bits is calculated by adding the length of respective data according to (10)

$$D = len\left(A\{c_{L,(1,2)}\}\right) + len\{A\{y\}\} + len\{A\{\phi\}\} + 2B_0, \qquad (10)$$

where $c_{L,(1,2)}$ are multiscaling coefficients, $y$ is a compressed measurement signal, $\phi$ is a sensing matrix, $A\{arg\}$ means arithmetic encoding, and $len\{arg\}$ is an operation that will return the length of the code. 2 times $B_0$ represents the DC offset information and the length of the compressed measurement signal. Another parameter used to evaluate the proposed method is the reconstruction error. Reconstruction error is evaluated with percentage root mean squared difference (PRD) given by (11)

$$PRD = 100\sum_{n=1}^{N}\frac{\|x_n - \hat{x}_n\|_2}{\|x_n\|_2}, \qquad (11)$$

where $x_n$ represents an original signal sample and $\hat{x}_n$ represents the reconstructed signal sample. The obtained error is a result of several factors. The first is the noise included in the MIT-BIH database. This noise is not present in the reconstructed signal, which influences the obtained error. The second factor is a quantization noise after quantization of the compressed measurement signal and multiscaling coefficients. And last is the error caused by the CS compression method.

All the tests to evaluate the proposed method were performed on the first channel of all MIT-BIH database records. The parameters used during the test are listed in Table 1.

*Table 1. Parameters used during the evaluation*

| Parameter | Value | Parameter | Value |
|---|---|---|---|
| $N$ | 2048 | $\max Q_{LB}\ level$ | 2 |
| $L$ | 3 | $\min Q_{LB}\ level$ | -2 |
| $dt$ | 0.03 | $\max Q_{HB}\ level$ | 0.5 |
| $B_{LB}$ | 6; 7 (64; 128 levels) | $\min Q_{HB}\ level$ | -0.5 |
| $B_{HB}$ | 6; 7 (64; 128 levels) | | |

where $B_{LB}$ is the number of bits used to quantize the low-frequency component of the ECG signal. Similarly $B_{HB}$ is the number of bits used to quantize the high-frequency component of the ECG signal. The max and min $Q_{LB}$ and $Q_{HB}$ levels represent the maximal and the minimal quantization level for respective ECG signal components. The evaluation was performed for seven Multiwavelets. For each Multiwavelet the evaluation was performed while using 6 and then 7 bits for quantization. The results are shown in Fig. 3.

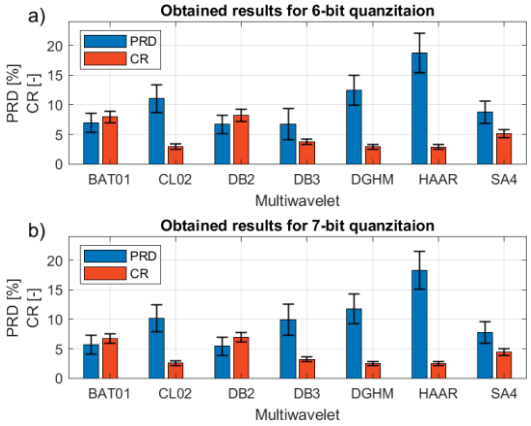


*Fig. 3. PRD and CR results for a) 6-bit quantization, b) 7-bit quantization*

As expected, the results for 7-bit quantization have lower CR and lower PRD than the results for 6-bit quantization. Lower PRD is the result of a smaller quantization error. From all Multiwavelets evaluated, DB2 and BAT01 Multiwavelets performed the best. Since DB2 Multiwavelet performed slightly better than BAT01 Multiwavelet, the next section will be focused on experiments performed with DB2 Multiwavelet.

The next experiment was focused on the influence of the quantization on the PRD and CR after reconstruction. This experiment was performed similarly to the previous

experiment but only with the use of DB2 Multiwavelet. The experiment was performed for 7 different numbers of quantization bits. The results are shown in Fig. 4.

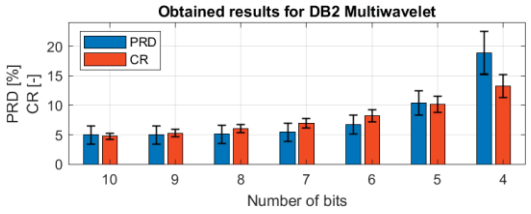


*Fig. 4. PRD and CR results for DB2 Multiwavelet*

Both PRD and CR were rising with the use of fewer bits for quantization. For the 10 to 8 bits used for quantization, the PRD change was less than 0.1 %. From 7 bits, the PRD started to exponentially increase. The CR was steadily increasing throughout the whole experiment. The best CR to PRD ratio was achieved by using 8-6 bits for quantization. For ECG signals the proposed method could operate at 8-6 quantization bits depending on the required PRD and CR. In the next section, a case study for chosen ECG record will be performed.

The visual comparison of the original ECG signal and reconstructed ECG signal for 6-bit and 7-bit quantization, with the use of DB2 Multiwavelet, is shown in Fig. 5.

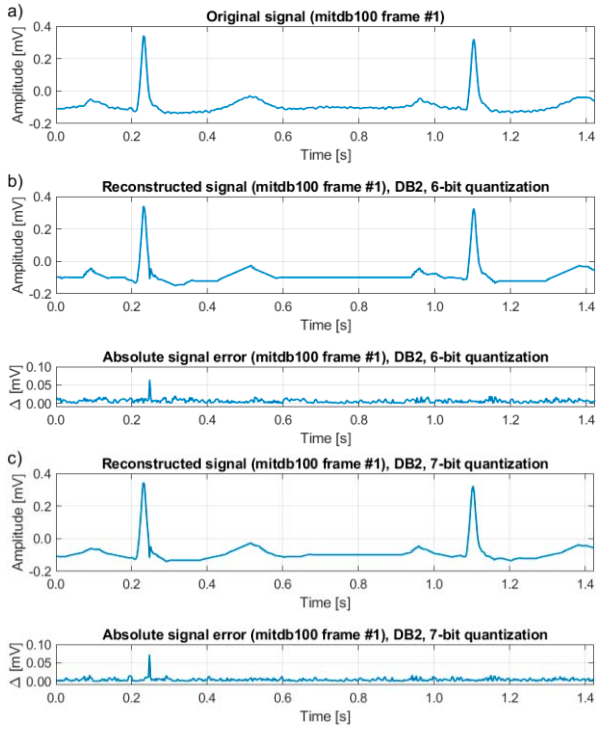


*Fig. 5. Case study of ECG frame #1 a) Original ECG signal, b) Reconstructed ECG signal with 6-bit quantization and absolute error, c) Reconstructed ECG signal with 7-bit quantization and absolute error*

In Fig. 5, the detail of two heartbeats from the first frame is shown. The reconstruction error is shown as well. The obtained results for the first frame with 6-bit quantization, shown in Fig. 5 b), were as follows. The calculated PRD after the signal reconstruction was 6.982 % and CR was 11.384. The obtained results for the first frame with 7-bit quantization, shown in Fig. 5 c), were as follows. The calculated PRD after the signal reconstruction was 4.966 % and CR was 9.422. The exact position of R waves of the heartbeat in Fig. 5 was in both cases included. The reconstruction error was mostly influenced by the quantization and by the noise which is present in the MIT-BIH database. The error after sparse signal reconstruction is present as well. The reconstructed signals in Fig. 5 are noiseless because the sparse signal recovery algorithms do not reconstruct the signal noise. The ECG signal in Fig. 5. c) is smoother than in Fig. 5. b). It is directly influenced by quantization. In both cases, there is an error around the 0.25-second mark. This error was caused by the signal reconstruction. But the error peak is lower than 80 µV which represents roughly 15 % error compared to peak to peak value of the ECG wave. Visually for the diagnostic, the error peak does not represent a significant error because it is a single value error. That peak error may be minimized by using more optimized method parameters.

The last experiment was focused on the frame transition and R wave amplitude change. The algorithm removes DC offset from the frame and then after reconstruction DC offset is restored. This can distort the transition between frames.

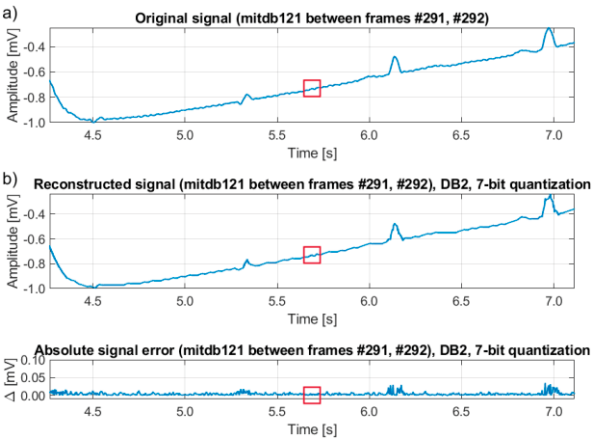


*Fig. 6. DC offset error case study a) Original ECG signal b) Reconstructed ECG signal with absolute error*

The distortion between the frames was present in the previously proposed method [13]. The method proposed in this article does not remove only the DC offset but removes the low-frequency component of ECG as well. Thus the distortion between the frames is minimal. This can be shown in the transition between the 291 and 292 frames of the mitdb121 record. The difference in DC offset is the biggest for this record. The detail of the transition between frames is shown in Fig. 6. The distortion is lower than 10 µV which is much less than in the previous method proposed in [13] where the DC offset error was more than 100 µV for the same record.

## V. CONCLUSION AND FUTURE WORKS

In this paper, a novel method of CS usable for ECG signals was introduced. The proposed method can reconstruct the ECG signal with sufficient quality to perform patient diagnostics while keeping high CR. The main advantage of the novel method is that it does not acquire prior information, patient-specific information, or any detector for ECG signal compression.

Future work is directed to: (i) evaluation of the method for different signals, (ii) evaluation of other Multiwavelets, (iii) evaluation of nonlinear quantization, (iv) searching for optimal configuration for the proposed method, (v) implementation of hardware prototype.

## ACKNOWLEDGMENT

The work is a part of the project supported by the Science Grant Agency of the Slovak Republic (No. 1/0413/22).

## REFERENCES

[1] S. Majumder, T. Mondal, and M. J. Deen, "Wearable Sensors for Remote Health Monitoring," *Sensors*, vol. 17, no. 1, Art. no. 1, Jan. 2017.

[2] N. El-Rashidy, S. El-Sappagh, S. M. R. Islam, H. M. El-Bakry, and S. Abdelrazek, "Mobile Health in Remote Patient Monitoring for Chronic Diseases: Principles, Trends, and Challenges," *Diagnostics*, vol. 11, no. 4, p. 607, Mar. 2021.

[3] S. C. Mukhopadhyay, "Wearable Sensors for Human Activity Monitoring: A Review," *IEEE Sens. J.*, vol. 15, no. 3, pp. 1321–1330, Mar. 2015.

[4] P. Klavík, A. C. I. Malossi, C. Bekas, and A. Curioni, "Changing computing paradigms towards power efficiency," *Philos. Transact. A Math. Phys. Eng. Sci.*, vol. 372, no. 2018, p. 20130278, Jun. 2014.

[5] M. Kumm, M. Hardieck, and P. Zipf, "Optimization of Constant Matrix Multiplication with Low Power and High Throughput," *IEEE Trans. Comput.*, vol. 66, no. 12, pp. 2072–2080, Dec. 2017.

[6] K. Sayood, *Introduction to Data Compression*. Morgan Kaufmann, 2017.

[7] D. L. Donoho, "Compressed sensing," *IEEE Trans. Inf. Theory*, vol. 52, no. 4, pp. 1289–1306, Apr. 2006.

[8] D. Craven, B. McGinley, L. Kilmartin, M. Glavin, and E. Jones, "Compressed Sensing for Bioelectric Signals: A Review," *IEEE J. Biomed. Health Inform.*, vol. 19, no. 2, pp. 529–540, Mar. 2015.

[9] P. Bera and R. Gupta, "Hybrid encoding algorithm for real time compressed electrocardiogram acquisition," *Measurement*, vol. 91, pp. 651–660, z 2016.

[10] L. De Vito, E. Picariello, F. Picariello, S. Rapuano, and I. Tudosa, "A dictionary optimization method for reconstruction of ECG signals after compressed sensing," *Sensors*, vol. 21, no. 16, 2021.

[11] M. Melek and A. Khattab, "ECG compression using wavelet-based compressed sensing with prior support information," *Biomed. Signal Process. Control*, vol. 68, 2021.

[12] J. Saliga, P. Dolinsky, I. Andras, and L. Michaeli, "A new CS method for ECG signal," in *24th IMEKO TC4 International Symposium and 22nd International Workshop on ADC and DAC Modelling and Testing (IMEKO TC-4 2020)*, Palermo, Italy, 2020, pp. 6–11.

[13] J. Šaliga, I. Andráš, P. Dolinský, L. Michaeli, O. Kováč, and J. Kromka, "ECG compressed sensing method with high compression ratio and dynamic model reconstruction," *Measurement*, vol. 183, p. 109803, Oct. 2021.

[14] G. B. Moody and R. G. Mark, "The impact of the MIT-BIH Arrhythmia Database," *IEEE Eng. Med. Biol. Mag.*, vol. 20, no. 3, pp. 45–50, May 2001.

[15] Y. C. Eldar and G. Kutyniok, Eds., *Compressed sensing: theory and applications*. Cambridge ; New York: Cambridge University Press, 2012.

[16] G. M. Fung and O. L. Mangasarian, "Equivalence of Minimal ℓ0- and ℓp-Norm Solutions of Linear Equalities, Inequalities and Linear Programs for Sufficiently Small p," *J. Optim. Theory Appl.*, vol. 151, no. 1, pp. 1–10, Oct. 2011.

[17] L. De Vito, F. Picariello, S. Rapuano, I. Tudosa, and L. Barford, "A Compressive Sampling-Based Channel Estimation Method for Network Visibility Instrumentation," *IEEE Trans. Instrum. Meas.*, vol. 69, no. 5, pp. 2335–2344, May 2020.

[18] F. Keinert, *Wavelets and Multiwavelets*, 1st edition. Boca Raton, FL: Chapman and Hall/CRC, 2003.

[19] J. Kromka, O. Kováč, and J. Šaliga, "Multiwavelet toolbox for MATLAB," in *2022 32nd International Conference Radioelektronika (RADIOELEKTRONIKA)*, Apr. 2022, pp. 01–05.

[20] A. Jensen and A. la Cour-Harbo, *Ripples in Mathematics*. Berlin, Heidelberg: Springer Berlin Heidelberg, 2001.

[21] "CVX: Matlab Software for Disciplined Convex Programming | CVX Research, Inc." http://cvxr.com/cvx/ (accessed Mar. 18, 2022).